M R S Internet Journal of Nitride Semiconductor Research

Volume 1, Article 40

Determination of the dislocation densities in GaN on c-oriented sapphire

A. Pelzmann, M. Mayer, C. Kirchner, D. Sowada, T. Rotter, Markus Kamp , K. J. Ebeling
Abteilung Optoelektronik, Universität Ulm

S. Christiansen, M. Albrecht, H. P. Strunk
Institut für Werkstoffwissenschaften, Lehrstuhl VII, Universität Erlangen-Nürnberg

B. Holländer, S. Mantl
Forschungszentrum Jülich, Inst. für Schicht-und Ionentechnik

This article was received on July 31, 1996 and accepted on December 16, 1996.

Abstract

We report on a comprehensive study of the defect structure in GaN grown on c-oriented sapphire by gas source molecular beam epitaxy and metal organic vapour phase epitaxy. Transmission electron microscopy is used to investigate the defect structures which are dominated by threading dislocations perpendicular to the sapphire surface and stacking faults. Additionally, dislocation densities are determined. For determination of dislocation densities by x-ray diffraction we employ a model that uses the linewidth of x-ray rocking curves for this purpose. Finally, Rutherford backscattering spectrometry is performed to complement the structural investigation.

1. Introduction

Group III Nitrides (e.g. AlN, GaN, InN and their alloys) are predestinated for optoelectronic applications from the long visible light range down to UV wavelengths since they cover a bandgap range from 1.6 to 6.2 eV. Nowadays, one of the most important optoelectronic applications of group III Nitrides are GaN based blue and green LEDs. High-brightness GaN based blue LEDs were first fabricated by S. Nakamura using c-oriented sapphire as substrate material and two-flow metal organic vapour phase epitaxy (MOVPE) for the epitaxial growth [1]. So far, best results in growth of high quality group III nitrides are achieved by MOVPE techniques. However, the growth of group III nitrides by gas source molecular beam epitaxy (GSMBE) using On Surface Cracking (OSC) of NH_3 appears also to be very promising [2] [3]. Particularly in our department we have the opportunity to compare both growth techniques directly since we are equipped with a MOVPE and a GSMBE system.

The lattice mismatch between sapphire and GaN is very large ($\Delta a/a$=16 %). 6H SiC is a more suitable substrate material for the epitaxial growth of GaN ($\Delta a/a$=3.5 %). However, due to the high price and the low availability of suitable 6H SiC, most groups use the less expensive sapphire for the growth of wurtzite-type nitrides. Due to the large mismatch of the lattice constants and the thermal expansion coefficients, GaN grown on sapphire has very high defect densities.

The first step in the fabrication of optoelectronic semiconductor devices is the optimization of the grown material referring to optical, electrical and crystalline quality. In our investigations we focus on transmission electron microscopy (TEM), Rutherford backscattering spectrometry (RBS) and high resolution x-ray diffraction (XRD) to examine the crystalline quality.

2. Experimental

2.1. Epitaxial growth

https://doi.org/10.1557/S109257830000212X Published online by Cambridge University Press

All layers make use of a AlN/GaN buffer with thicknesses of a few nanometers before the GaN layer is grown. For GSMBE growth we use an almost standard MBE system (Riber32) adapted to group V gas sources. The system is turbo pumped. The attached gas control and handling system is home made. NH_3 is introduced into the system through a standard high temperature injector (Riber HTI 432). Effusion cells are used to supply the group III species Ga and Al. The GaN layers are grown at growth rates of 700 nm/h to a thickness of approximately 2 μm. The MOVPE system is an AIXTRON AIX 200 RF. It is equipped with a water cooled quartz glass reactor. Substrates (up to 2 inch) are loaded on a SiC-coated graphite susceptor with a rotating disc. An RF heating allows process temperatures up to 1200 °C. The growth pressure is 100 mbar; nitrogen is used as carrier gas.

2.2. TEM, x-ray diffraction and RBS

The microstructural characterization (in plane view and cross-section) is based on conventional transmission electron microscopy in a Philips CM30, operated at 300 kV and high resolution (HR) TEM in a Philips CM300 UT, operated at 300 kV (spherical aberration Cs = 0.65 mm and a point-to-point resolution of 1.65 Å). The cross-sectional specimens are prepared by conventional mechanical grinding and dimpling with diamond paste, followed by ion milling with Ar^+ to electron transparency in a Gatan duomill (operated at 4.5 kV, 1 mA, 13°, nitrogen cooling stage). For x-ray rocking curve measurements we use a Philips 5 crystal diffractometer ($Cu_{K\alpha 1}$ line) with a Bartels monochromator. All measured reflections are optimized for maximum intensity by rotating the ψ and the Φ angles. Rutherford back scattering is performed with 2.0 MeV He^+ ions at a scattering angle of 170°.

3. Theoretical model for x-ray analysis of threading dislocations

A model described by Ayers [4] uses the x-ray linewidth broadening due to threading dislocations (TD) for calculation of their densities. Following the model of Ayers, we assume that the x-ray rocking curve peaks are Gaussian in shape and the linewidth represents a convolution of the following contributions: the intrinsic rocking curve width β_0, the intrinsic rocking curve width for the Bartels monochromator β_d, the rocking curve broadening due to angular rotation at dislocations β_α, the broadening caused by strain surrounding dislocations β_ε, the rocking curve broadening due to crystal size β_L, and the broadening due to curvature of the crystal β_r. Thus the square of the measured rocking curve linewidth β_m is given by [4]:

$$\beta_m^2(hkl) = \beta_0^2(hkl) + \beta_d^2(hkl) + \beta_\alpha^2(hkl) + \beta_\varepsilon^2(hkl) + \beta_L^2(hkl) + \beta_r^2(hkl) \quad (1)$$

The intrinsic rocking curve width is calculated by [5]:

$$\beta_0 = 2.12 \cdot \left(\frac{e^2}{m \cdot c^2}\right) \cdot \frac{N \cdot \lambda^2 \cdot |F_{hkl}|}{\pi \sin(2 \cdot \theta)} \left(\frac{1 + |\cos(2 \cdot \theta)|}{2}\right) \cdot \left(\frac{\sin(\theta_1)}{\sin(\theta_2)}\right) \quad (2)$$

Where θ is the Bragg angle, θ_1 and θ_2 are the angles of the primary and the reflected x-ray beams, λ is the wavelength and F_{hkl} is the structure factor. The contributions β_α and β_ε are calculated by [4]:

$$\beta_\alpha^2 = 2 \cdot \pi \ln(2 \cdot b^2 \cdot D) =: K_\alpha \quad (3)$$

$$\beta_\varepsilon^2 = 0.09 \cdot b^2 \cdot D \cdot \left| \ln(2 \cdot 10^{-7}\,\mathrm{cm} \cdot \sqrt{D}) \right| \cdot \tan^2\theta =: K_\varepsilon \cdot \tan^2\theta \quad (4)$$

where b is the length of the burgers vector, D is the dislocation density and K_α and K_ε are introduced to simplify equations 3 and 4 . Equation 4 is valid for pure screw dislocations, but the actual character of the TD will have only weak effect on strain broadening [4]. Therefore equation 4 was taken for our calculations. Broadening due to crystal size β_L can often be neglected for layers thicker than 1μm [4]. The broadening due to curvature β_r can be estimated by comparison of the substrate rocking curves before and after growth of a layer. For our samples the effect of broadening due to curvature yields a few arcseconds and can therefore be neglected. Thus equation 1 simplifies to:

https://doi.org/10.1557/S109257830000212X Published online by Cambridge University Press

$$\beta_m^2(hkl) \approx \beta_0^2(hkl) + \beta_d^2(hkl) + K_\alpha + K_\varepsilon \cdot \tan^2\theta \quad (5)$$

Since β_0 can be calculated according to equation 2, β_m is the measured linewidth and β_d is constant we now introduce the adjusted linewidth β_{adj} to simplify the relation.

$$\beta_{adj}^2 := \beta_m^2(hkl) - \beta_0^2(hkl) - \beta_d^2(hkl) \quad (6)$$

Plotting β_{adj}^2 for at least three different x-ray reflections versus $\tan^2\theta$ should yield a straight line. The dislocation densities can then be independently calculated from the slope as well as the intercept of that line. For internal consistency the results should be identical.

4. Results and discussion

TEM measurements of both MOVPE and GSMBE samples showed large numbers of TD perpendicular to the sapphire substrate. Additionally, large amounts of plane defects and stacking faults were observed. Figure 1 and figure 2 show a cross sectional view of a GSMBE sample and a plane view of a MOVPE one. The observed TD have pure screw and edge character with burgers vectors **b** in ± [0 0 0 1] directions for the screw and $\frac{1}{3}\langle 2\bar{1}\bar{1}0 \rangle$ for the pure edge dislocations. Also mixed TD were found with burgers vectors **b** in $\frac{1}{3}\langle \bar{1}\bar{1}23 \rangle$ directions. Additionally, HRTEM showed regions tilted by an angle of 60° with regard to the sapphire substrate. These tilted regions are attributed to islands in the AlN buffer layer, which grow tilted to reduce the stress by the lattice mismatch (This results will be puplished elsewhere). The dislocation densities counted from the cross section TEM micrographs lie in the range among 10^9 to 10^{10} per cm^2 for the GSMBE and MOVPE samples. The obtained information about the defect structure and the dislocation densities can be taken to prove if it is possible to determine quantitative values for dislocation densities in heteroepitaxially grown GaN by x-ray diffraction. For this purpose we employed the theoretical model described above. TEM micrographs of the GSMBE sample used for x-ray measurements show 3×10^9 TD/cm^2 with screw and edge dislocations in the same order of magnitude and additionally large amounts of plane defects. The MOVPE sample taken for the x-ray measurements has 3.5×10^8/cm^2 screw dislocations, 6×10^9/cm^2 edge dislocations and no plane defects, which was also observed by TEM.

We measured 3 symmetric and 3 asymmetric reflections of each sample. Figure 3 and figure 4 show the plots according to equation 6 for various x-ray peaks. In both cases the symmetric and the asymmetric reflections are not on a single straight line as predicted by the model. Because of the obvious separation of the data in figure 3 and figure 4 the linear fits were separately employed on the symmetric and the asymmetric reflections for each sample. Table 1 shows the dislocation densities calculated according to the Ayers model from slopes and intercepts of these linear fits shown in figure 3 and figure 4. TEM data are given for comparison.

Since the calculated dislocation densities vary significantly, there is a lack of internal consistency when the Ayers model is applied. For the GSMBE sample internal consistency can just be achieved for the results belonging to the symmetrical reflections but the calculated dislocation densities are an order of magnitude lower than the results achieved by TEM. It is not yet understood clearly why the strong separation of the x-ray linewidths appears in both samples. A possible explanation comes out of the real defect structure examined by TEM, where we found stacking faults and other plane defects in addition to the TD in the GSMBE sample. Stacking faults can have a major influence on the strong separation of symmetric and asymmetric linewidths because they create crystal regions with small coherence length perpendicular to the substrate. Stacking faults and other kinds of plane defects however are not included into the Ayers model, which takes only the effect of pure TD into account.

Heying et al. reported that the symmetric (00.2) reflex is broadened by screw or mixed TD, whereas the asymmetric (10.2) reflex is broadened by all TD [6]. All the measured asymmetric reflections of our MOVPE sample have broader linewidth compared to the symmetric ones (figure 4). The comparison of the real defect structure gained by TEM with this x-ray results shows that the reason for the different broadening of the peaks must be the same as reported by Heying. For the MOVPE sample internal consistency that is demanded in the Ayers model is just fulfilled for the results of the asymmetric data. Here, the calculated dislocation densities correspond to the density of screw

https://doi.org/10.1557/S109257830000212X Published online by Cambridge University Press

dislocations determined by TEM and not to the total amount of threading dislocations. This is contradictory to Heyings finding and to our TEM results. The specific dislocation structures in heteroepitaxial GaN can lead to anomalously low symmetric rocking curve linewidths [6]. For accurate determination of the dislocation densities in heteroepitaxial GaN with the Ayers model this anomalous lowering must be taken into account by modification of the used equations. With our GSMBE sample (figure 3) we observe asymmetric reflections with linewidths smaller than the symmetric ones. This is in contrast to Heyings hypothesis and reveals that the broadening can not only be explained by the ratio of the density of screw to total TD. As mentioned above we propose that plane defects (such as stacking faults) have to be considered, too.

Our x-ray results compiled in figure 3 and figure 4 clearly show that it is not sufficient to measure a single reflex for crystalline optimization. The Ayers model predicts that it should be sufficient to measure three different reflections (symmetric or asymmetric), assuming that the defect structure is determined by TD. We showed that the whole defect structure has to be considered since in GaN beside TD, plain defects are also present, giving significant differences in the defect densities determined from symmetric and asymmetric reflections.

Anyhow, the Ayers model which has proven its validity for different material systems and for GaN bulk crystals [7], is also useful to GaN since it gives indications on the actual defect structure namely if the crystal contains only TD or if other defects are present in addition.

In addition to TEM and x-ray diffraction, RBS and ion channeling measurements were performed to investigate the crystalline perfection of the GaN layers. Figs. 5 and 6 show random RBS and [0 0 0 1] channeling spectra of the GSMBE and MOVPE samples. In the case of the MOVPE sample, the backscattering contribution of N is superimposed on the Al and O contribution of the substrate below channel 400. In the case of the GSMBE sample, the backscattering contribution of the substrate cannot be detected because of the large layer thickness. The GSMBE grown sample exhibits a channeling minimum yield of only 1.2 % indicating a very good crystalline quality. In comparison, the MOVPE sample shows a minimum yield of 3.0 % and a considerable dechanneling with increasing depth, indicating a significantly higher density of structural defects, especially near the interface to the substrate. Further planar dechanneling measurements are necessary to improve the sensitivity for TD perpendicular to the surface.

5. Conclusion

TEM investigations clearly showed the defect structure of our MOVPE and GSMBE grown GaN. Dislocation densities were estimated by TEM cross sections to be in the range between 3×10^9 to $6\times10^9/cm^2$. A theoretical model for quantitative calculation of dislocation densities from x-ray rocking curve linewidths was applied to the data obtained by our x-ray measurements. The results showed that the employed Ayers model must be modified for stacking faults and other plane defects to give accurate determination of TD densities. Furthermore, anomalous lowering of symmetric reflections in heteroepitaxial GaN also has to be considered when applying the Ayers model on samples with pure TD defect structure. Additionally, our rocking curve analysis showed that optimization on the crystalline quality with symmetric reflections is not sufficient. The asymmetric reflections must also be taken into account. RBS/channeling revealed astonishing low minimum yield of 1.2 % for the GSMBE grown sample (which is comparable to GaAs homoepitaxy) in spite of the high dislocation density. Further investigations in different crystal orientations have to be accomplished to gain a deeper understanding of the RBS data.

Acknowledgments

The authors want to thank Dr. Nikolaus Herres and Dr. M. Leszczynski for helpful discussion on x-ray diffraction and the Bundesministerium für Bildung und Forschung for financial support.

References

[1] S. Nakamura, T. Mukai, M. Senoh, *J. Appl. Phys.* ***76***, 8189 (1994).

[2] M. Kamp, M. Mayer, A. Pelzmann, S. Menzel, C. Kirchner, H. Y. A. Chung, H. Sternschulte, K. J. Ebeling, unpublished (1996).

[3] M. Kamp, M. Mayer, A. Pelzmann, A. Thies, H. Y. Chung, H. Sternschulte, O. Marti, K. J. Ebeling, *Mater. Res. Soc. Symp. Proc.* ***395***, 135-139 (1996).

[4] J. E. Ayers, *J. Cryst. Growth* ***135***, 71-77 (1994).

https://doi.org/10.1557/S109257830000212X Published online by Cambridge University Press

[5]B. E. Warren, *"X-Ray Diffraction"*, (Addison-Wesley, Reading, MA, 1969).

[6] B. Heying, X. H. Wu, S. Keller, Y. Li, D. Kapolnek, B. P. Keller, S. P. DenBaars, J. S. Speck, *Appl. Phys. Lett.* ***68***, 643-645 (1996).

[7]M. Leszczynski (High Pressure Research Center, Warsaw, Poland): Private communication

Table 1

	GSMBE A1 disloc. dens. (cm-2)	MOVPE B2 disloc. dens. (cm-2)
slope (symm. reflections)	3×10^{8}	2×10^{8}
intercept (symm. reflections)	8×10^{8}	1×10^{7}
slope (asymm. reflections)	1×10^{7}	2×10^{8}
intercept (asymm. reflections)	3×10^{8}	3×10^{8}
TEM, screw dislocations	1.5×10^{9}	3×10^{8}
TEM, edge dislocations	1.5×10^{9}	6×10^{9}
TEM, total amount of TD	3×10^{9}	6.3×10^{9}
TEM, other defects	large amounts of stacking faults and twins	no plain defects

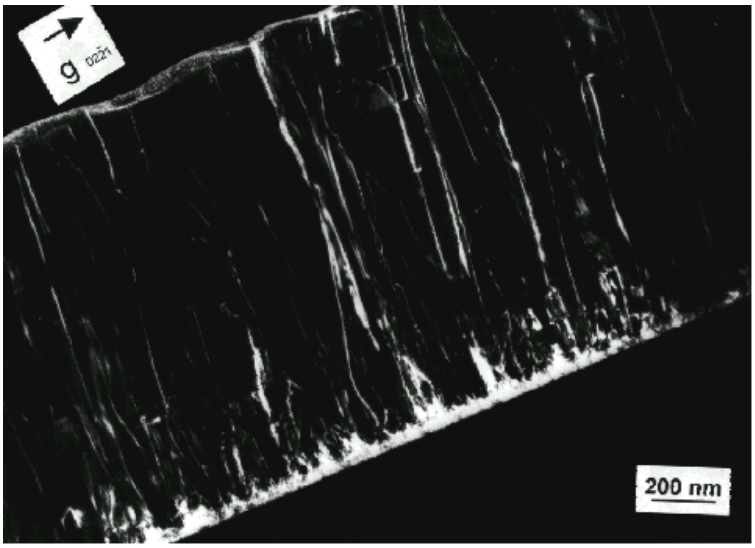

Figure 1. TEM cross section of a GSMBE grown GaN sample

https://doi.org/10.1557/S109257830000212X Published online by Cambridge University Press

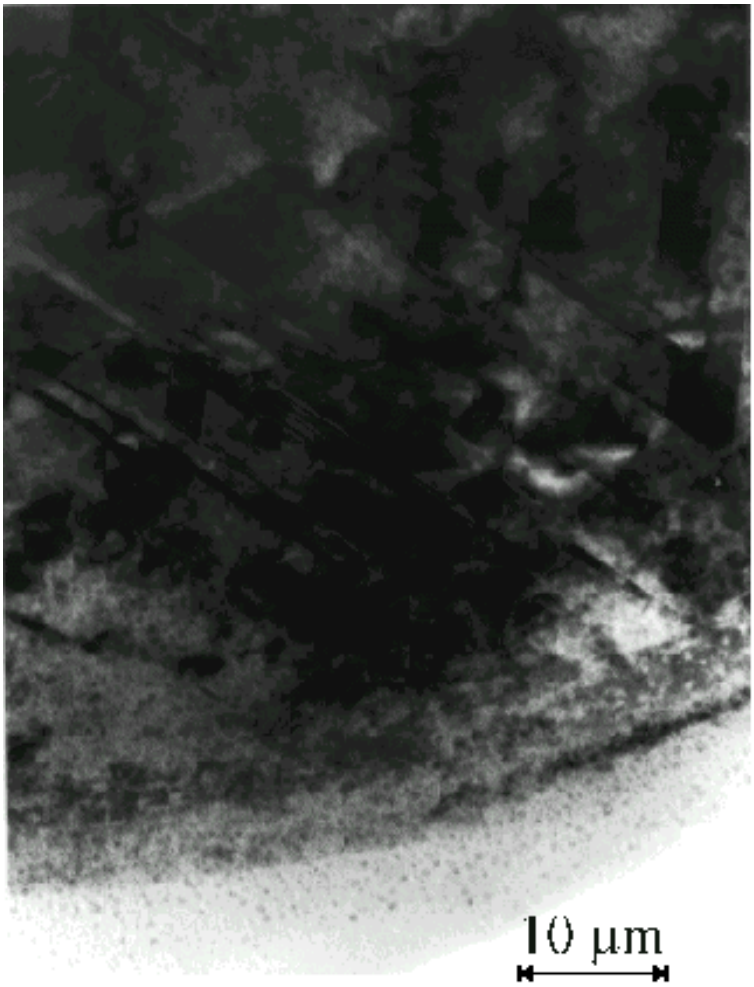

Figure 2. TEM plane view of a MOVPE grown sample

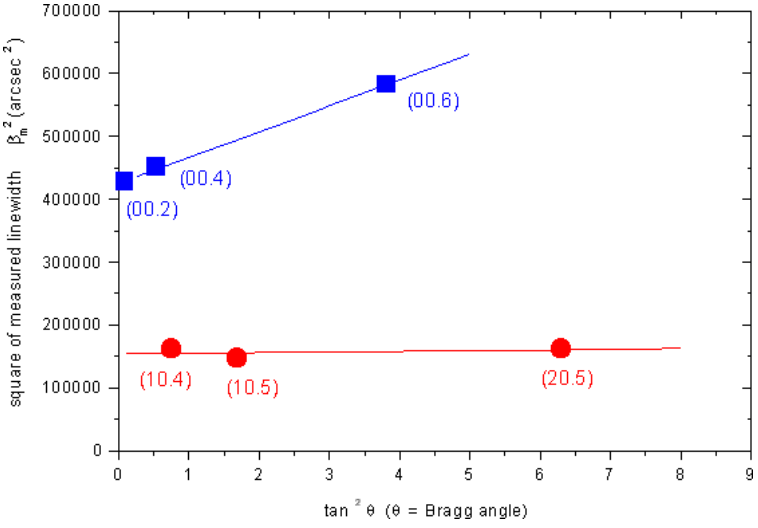

Figure 3. Plot according to Ayers model (GSMBE)

https://doi.org/10.1557/S109257830000212X Published online by Cambridge University Press

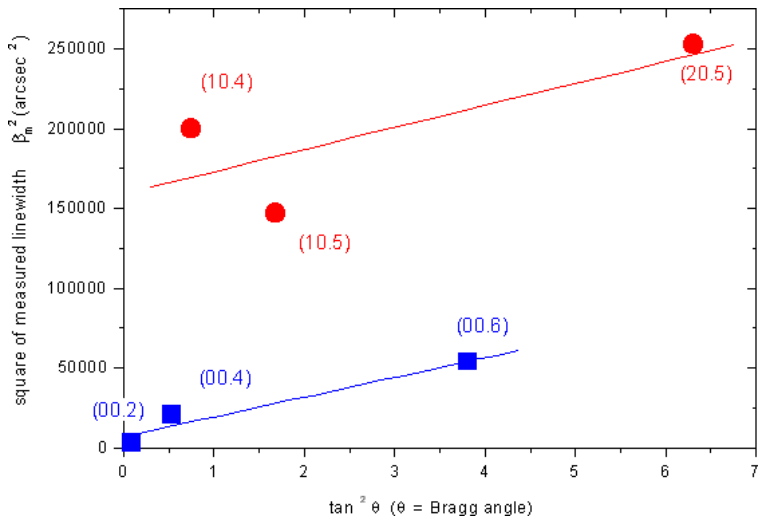

Figure 4. Plot according to Ayers model (MOVPE)

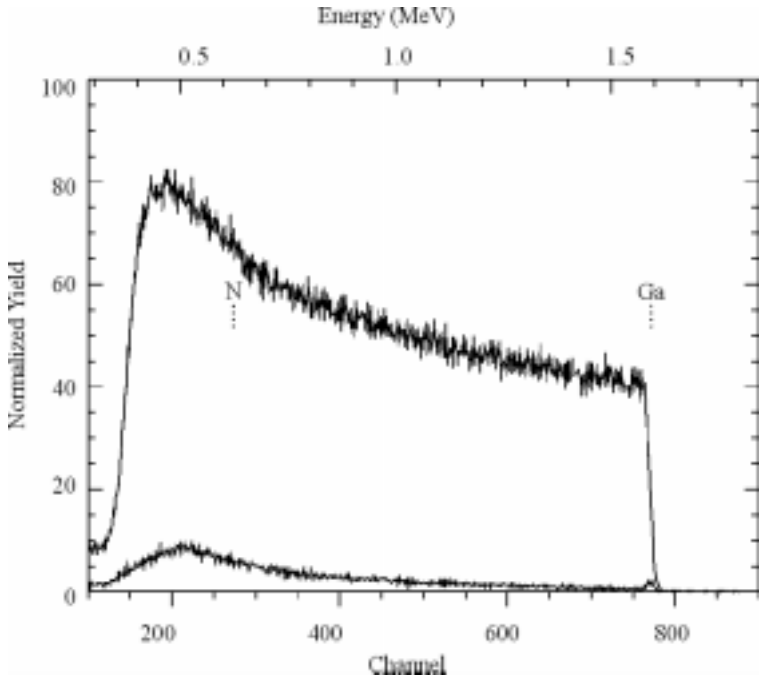

Figure 5. RBS of GSMBE grown GaN

https://doi.org/10.1557/S109257830000212X Published online by Cambridge University Press

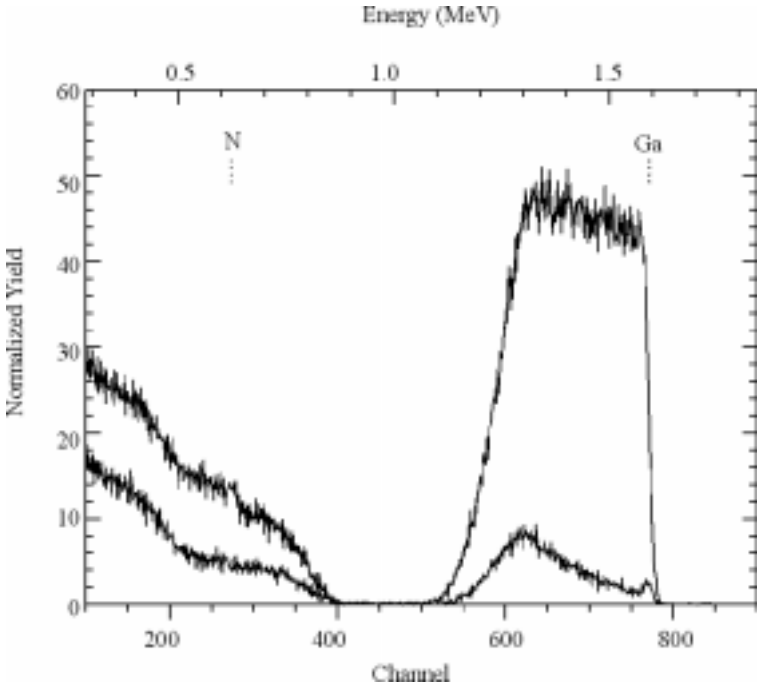

Figure 6. RBS of MOVPE grown GaN

M R S Internet Journal of Nitride Semiconductor Research

https://doi.org/10.1557/S109257830000212X Published online by Cambridge University Press